

THE OPTIMIZATION OF THE NUMBER OF PAINTS FOR ADEQUATE FIELD
COVERAGE IN A UNIFORM SCANNING PROTON BEAM

A RESEARCH PAPER

SUBMITTED TO THE GRADUATE SCHOOL

IN PARTIAL FULFILLMENT OF THE REQUIREMENTS

FOR THE DEGREE

MASTER OF ARTS

BY

SEAN BOYER

DR. RANJITH WIJESINGHE, PH.D – ADVISOR

BALL STATE UNIVERSITY

MUNCIE, INDIANA

JULY 2013

Abstract

RESEARCH PAPER: The Optimization of the Number of Paints for Adequate Field Coverage in a Uniform Scanning Proton Beam

STUDENT: Sean Boyer

DEGREE: Master of Arts

COLLEGE: Sciences and Humanities

DATE: July 2013

PAGES: 27

Uniform scanning proton beams work by scanning a pencil-beam of radiation throughout the entire area of the treatment field. Specifically for Princeton Procure Management, LLC in Somerset, NJ (ProCure NJ), the beam is scanned at 30 hertz (Hz) in the vertical direction, and 3 Hz in the horizontal direction. The time it takes for one “paint” in the 30 Hz x 3 Hz scanning pattern is 1/3 of a second ($3\text{Hz} = 3 \text{ revolutions per second} = 1 \text{ second per } 3 \text{ revolutions}$). Currently, the first layer of the treatment field is set to “paint” the entire treatment field 40 times. The number 40 has been chosen somewhat arbitrarily. If the number of paints is reduced, it will decrease patient treatment time, leading to less patient movement during beam-on time.

Field parameters such as the flatness and symmetry need to be checked for patient safety. This hypothesis will be explored through a MATLAB simulation, as well as beam data taken at ProCure NJ. To measure beam data, the IC ProfilerTM Model 1122 will be used. This IC ProfilerTM uses 4 simultaneous linear arrays of ion chambers; X and Y axes with 5mm spacing, plus two diagonal axes with 7.07mm spacing. The “passing rate” will be defined by how often a certain field is within tolerance for flatness and symmetry in both the x and y axes.

The results show that the simulation matches well with measurements for 40 paints (76% vs. 80% passing rate), but not as closely for 30 paints (58% vs. 80% passing rate). Regardless of the number of paints, the measurements showed that the highest range failed flatness and all of lower ranges passed flatness and symmetry on all measurements.

Because of the small sample size, it is difficult to determine the effect of the number of paints on the flatness and symmetry. If more data could have been taken at different ranges and numbers of paints, it is possible a stronger trend could have been found. The measurements indicate that there is a stronger relation between range and passing rate, rather than number of paints and passing rate. The simulation only models the number of paints. Creating a simulation that models range is beyond the scope of this paper. Future studies should include more measurements at different ranges and numbers of paints.

Acknowledgements

First, I would like to thank my mother, who was a constant source of inspiration and motivation to complete this project. I would like to thank my father for his generosity throughout my long college career. I would like to thank Shenna, for all of her understanding during my long days and nights as a student. I would like to thank my research advisor, Dr. Ranjith Wijesinghe, for his patience and guidance throughout this long journey.

TABLE OF CONTENTS

	PAGE
ABSTRACT	ii
ACKNOWLEDGEMENTS	iv
TABLES OF CONTENTS.....	v
CHAPTER ONE: Introduction.....	1
1.1 The Bragg Peak.....	2
1.2 The Beam Path.....	6
1.3 Number of Paints.....	7
CHAPTER TWO: Materials and Methods.....	10
2.1 Beam Size.....	10
2.2 Simulation.....	12
2.3 Flatness and Symmetry.....	15
2.4 Measurements.....	16
CHAPTER THREE: Results.....	18
3.1 Simulation.....	18
3.2 Measurements.....	20
CHAPTER FOUR: Discussion.....	23
4.1 Measurement Versus Simulation.....	23
4.2 The Influence of Range	24
CHAPTER FIVE: Future Studies.....	26
CHAPTER SIX: References.....	27

List of Figures

Figure 1.1	Bragg Peak. A visualization of the dose deposited to tissue by an energetic proton	3
Figure 1.2	Spread Out Bragg Peak (SOBP). A visualization of multiple Bragg Peaks with decreasing energy. Curve one is the summation of all Bragg Peaks, the SOBP. Curve two is the Bragg Peak that defines the range of the SOBP. Curve three, and the subsequently smaller curves, are the Bragg Peaks that add up to the SOBP. [1]	4
Figure 1.3	Range Compensator. A device that will be inserted into the treatment field on the end of the snout. The compensator shapes the distal edge of the treatment field	5
Figure 1.4	Aperture. The aperture is a device that will be inserted into the treatment field on the snout. The aperture shapes the lateral edges of the treatment field	6
Figure 1.5	Proton Path. The proton accelerates to the appropriate energy (about 230 MeV at ProCure NJ), and then exits the cyclotron into the beamline. The beamline directs the protons to the degrader, where the energy of the protons is reduced to the desired energy. The protons proceed through the beamline to the selected room, where they enter the snout. The snout uses scanning magnets to bend the protons in the horizontal and vertical direction. For wobbling, the protons are scanned in a repeating pattern. The protons will hit the aperture and compensator, shaping the protons to the target dimensions.	7
Figure 1.6	Scanning pattern. The protons are scanned at 3Hz in the horizontal direction, 30Hz in the vertical direction.	8
Figure 2.1	Simulated Beam. Above is a beam from the MATLAB simulation, with red signifying the maximum radiation (a value of ~1 in the program) and the blue signifying the minimum radiation.	11
Figure 2.2	Untrimmed Field. The treatment field after scanning the beam across it 40 times. Red signifies the maximum radiation, blue signifies the minimum. In this case, the treatment field was represented by a 540x540 cell matrix. The axes seen above are the position in the treatment field matrix.	13
Figure 2.3	Trimmed Field. The treatment field after scanning the beam across it 40 times. Red signifies the maximum radiation, blue signifies the minimum. Although the field appears to be noisy,	15

it is not. The calculated flatness and symmetry is within the specified tolerance (less than 2% symmetry, less than 3% flatness). This time, the inner portion of the field was copied to a new matrix to properly analyze the flatness and symmetry.

Figure 3.1	Number of Paints vs. Passing Rate. The above figure shows the number of paints on a layer vs. the percentage of simulations that passed.	20
Figure 3.2	X and Y Flatness of 30 vs. 40 paints on the first layer.	22
Figure 3.3	X and Y Symmetry of 30 vs. 40 paints on the first layer.	23

List of Tables

Table 2.1	The range and modulation values chosen for this study.	18
Table 3.1	Number of Paints, Passing Rate	19

Chapter 1

Introduction

In external beam proton therapy, there are two general ways of delivering a beam of protons to the target: scattering and scanning [1]. A scattering proton beam will direct a narrow beam of protons onto a scatterer, which will make the protons scatter in all directions. A snout, or collimating device, will collimate the protons into a suitable field for treatment. Scattering allows the protons to reach the necessary field size to treat a target or patient. This scattering technique is very similar to external beam photon therapy. In a linear accelerator, a beam of high-energy electrons will be directed onto a flattening filter [2], which corresponds to a scatterer in proton radiotherapy. Again, the beam will need to be collimated so that photons mainly escape in the preferred direction. Unfortunately, the scattering technique causes beam losses and energy degradation of the therapeutic beam [3].

In external beam proton radiotherapy, there is another treatment technique known as scanning. The scanning technique does not require a scatterer to spread out the protons to the proper field size. Unlike photons, protons are charged particles, which can be directed using magnets. A general scanning beam system uses magnets to control where the protons go and can

scan each voxel of a treatment field nearly independently. A simpler version of this, called Wobbling, scans a constant-intensity pencil beam over a pattern many times to create a uniform radiation field [3]. Two advantages of this system are that the protons do not lose any energy from scattering, and they will not produce unwanted scattered radiation because of the scatterer. In a scattering system, the scatterer serves two purposes: to select the proper energy for the beam, and to scatter the beam to the required field size. A large field size requires a lot of material to scatter the beam, whereas a large energy requires a small amount of material, so as to not reduce the energy too much. Therefore, delivering large fields and high energies in scattering beams has certain limitations, whereas scanning beams do not have the same problem. Also, having a scatterer near the patient will lead to unwanted radiation coming directly from the scatterer; obviously this is not a problem with a scanning beam, as there is no scatterer to produce this unwanted radiation.

1.1 The Bragg Peak

Proton therapy makes use of the Bragg Peak to optimize dose conformity around a target. The Bragg Peak defines how a proton loses its energy along its path. When an energetic proton enters a medium, it will slowly begin to slow down because of Coulombic interactions. These interactions will produce ionizations in the medium, leading to energy from the proton being deposited to the medium. As the proton speed decreases, the energy deposited increases. If the proton spends the first half of its kinetic energy along the pathlength x , the remaining half of the energy will be spent in the distance $\approx x/3$ [4], results in the Bragg Peak is visualized below:

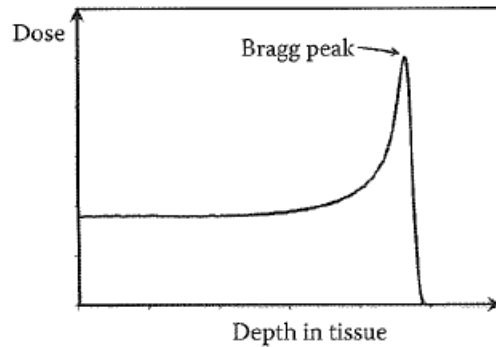


Figure 1.1 Bragg Peak. A visualization of the dose deposited to tissue by an energetic proton. [1]

This large loss of energy close to the end of the proton's path produces a spike in energy deposited to the medium at the end of its path. This will distribute negligible energy past this point. The path length (or Range) of the proton depends on its initial energy. The International Commission on Radiation Units & Measurements Report 78 (ICRU 78) defines the range as the depth along the beam central axis in water to the distal 90% point of the maximum dose value [4]. By controlling the initial energy of protons, the energy distribution to a medium can be optimized to a desired path length. Unfortunately, a mono-energetic proton beam is too narrow to give uniform dose to a tumor of any significant size; therefore the Bragg Peak must be spread out to cover the entire target [5]. The spread of the Bragg Peak will be referred to as the Spread Out Bragg Peak (SOBP). The SOBP is seen below:

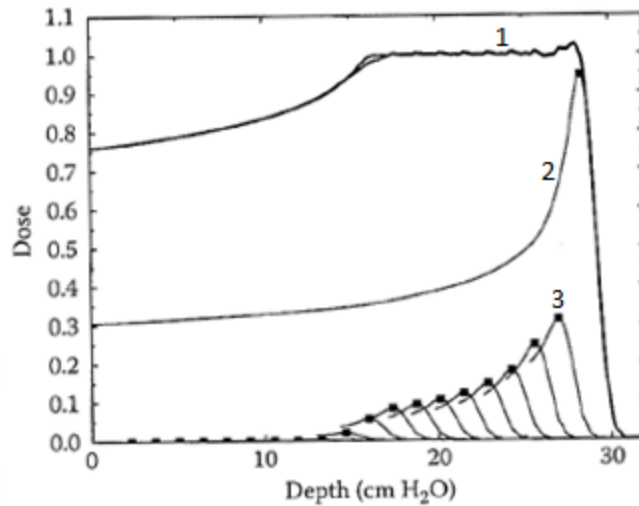


Figure 1.2 Spread Out Bragg Peak (SOBP). A visualization of multiple Bragg Peaks with decreasing energy. Curve one is the summation of all Bragg Peaks, the SOBP. Curve two is the Bragg Peak that defines the range of the SOBP. Curve three, and the subsequently smaller curves, are the Bragg Peaks that add up to the SOBP. [1]

The SOBP can be optimized so that the protons deliver their max energy only to the target, and leave the medium beyond the target unscathed. The area under the Spread Out Bragg Peak is called the Beam Modulation. The part of the curve before the peak is called the Build-Up Region. ICRU 78 defines the SOBP length, or the modulation, as the distance in water between the distal and proximal 90% points of the maximum dose value [4]. At Princeton ProCure Proton Center in Somerset, New Jersey (ProCure NJ), the modulation is defined as the distance between the 95% points of the maximum dose value. The reason for this deviation from the standard definition is the way that the SOBP is measured. For large SOBPs, where the modulation is approaching the range, the build-up region dose can become greater than 90% of the maximum dose. This is because it will take many individual Bragg Peaks to contribute to the

SOBP part of the curve, but this will also increase the Build-Up Region. When this large build-up region appears, it can be very difficult to distinguish this region from the SOBP. In these cases, it may help to define the SOBP as the peak between the proximal and distal 95%, instead of the 90%.

When “building” an SOBP, the different segments of that SOBP may be referred to as “layers” or “energy layers”. Typically, the protons will go through an aperture, which molds our field to a specific two-dimensional shape from the perspective of the Beam’s Eye View (BEV). The aperture will shape the two lateral dimensions of the field. Energy stacking will control that third dimension of the field, which is the depth. The depth of the field will be further shaped by a “range compensator”, which is a wax block with varying height to conform to the shape of the target. Figures of these are shown below:

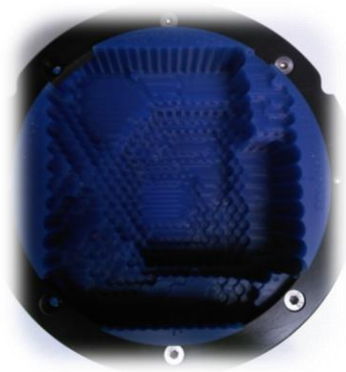


Figure 1.3 Range Compensator. A device that will be inserted into the treatment field on the end of the snout. The compensator shapes the distal edge of the treatment field



Figure 1.4: Aperture. The aperture is a device that will be inserted into the treatment field on the snout. The aperture shapes the lateral edges of the treatment field.

1.2 The Beam Path

At ProCure NJ, a cyclotron is used to deliver the protons to the patient. The cyclotron accelerates the protons to roughly 230 MeV, and then releases the protons into the beamline. In the beamline, a “degrader” will reduce the energy of the protons down to the necessary level for patient treatment. The protons will then go through the beamline to the chosen treatment room, where the energy will be further fine-tuned in energy and location. Once the energy and location of the beam of protons is within tolerance, this beam will be allowed to go into the patient room via the “snout”. The snout is essentially a transport device for protons between the beamline and the patient. The snout will hold an aperture to shape the beam in the BEV. Downstream of the aperture, the snout will also hold a wax compensator. This compensator will shape the distal edge of the beam. A diagram of the proton path is shown below:

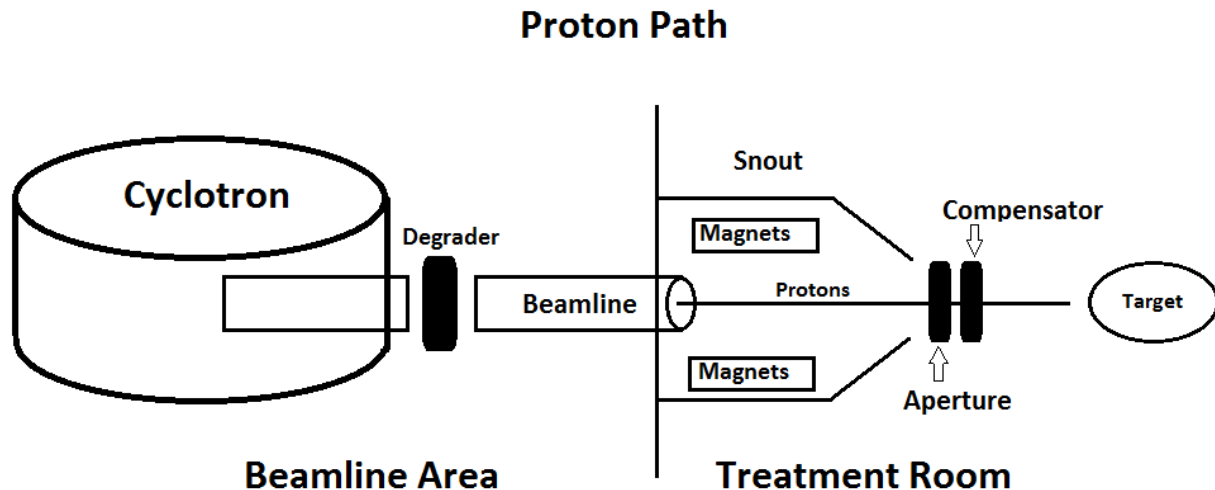
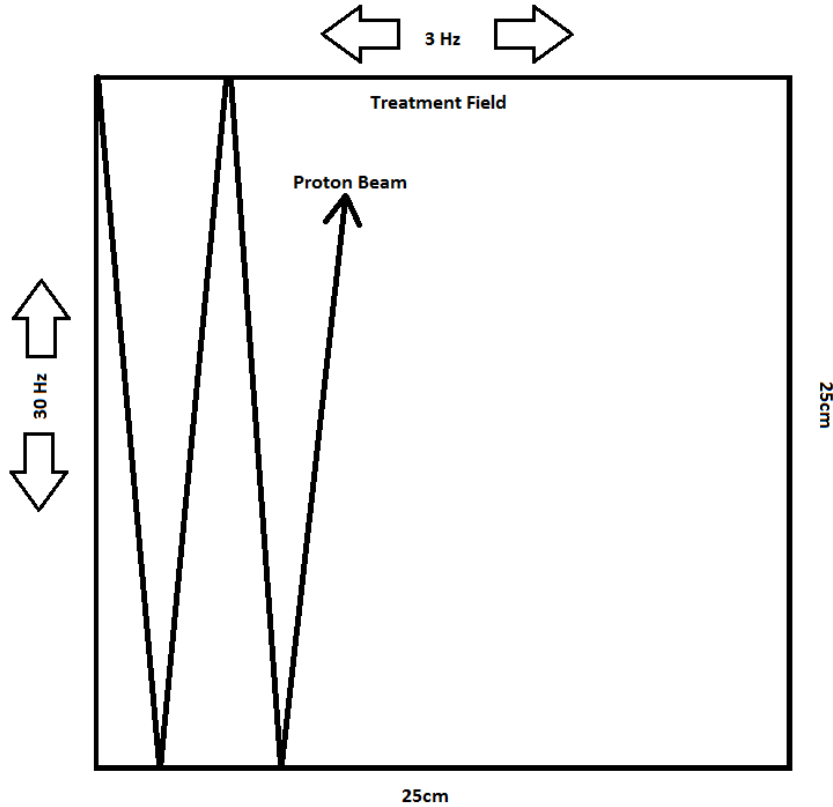


Figure 1.5 Proton Path. The proton accelerates to the appropriate energy (about 230 MeV at ProCure NJ), and then exits the cyclotron into the beamline. The beamline directs the protons to the degrader, where the energy of the protons is reduced to the desired energy. The protons proceed through the beamline to the selected room, where they enter the snout. The snout uses scanning magnets to bend the protons in the horizontal and vertical direction. For wobbling, the protons are scanned in a repeating pattern. The protons will hit the aperture and compensator, shaping the protons to the target dimensions.

1.3 Number of Paints

At ProCure NJ, a wobbling beam is used to treat patients. This wobbling beam simultaneously scans the protons horizontally at 3 hertz (Hz) and vertically at 30 hertz (Hz), as shown below:



*Picture NOT to scale

Figure 1.6 Scanning pattern. The protons are scanned at 3Hz in the horizontal direction, 30Hz in the vertical direction.

A “paint” is defined by the beam going to one field edge, back to the other field edge, and ending at the original position. At ProCure NJ, the lower scanning field speed is 3 Hz. Therefore, one paint takes 1/3 of a second, or 1 revolution per 3 seconds. The first layer of all patient treatments at ProCure NJ currently receives 40 paints. This number of paints has been shown to produce flatness and symmetry within our specified tolerances for patient treatment fields (Flatness $\leq 3\%$, Symmetry $\leq |2\%|$). The number of paints was chosen somewhat arbitrarily, and the minimum number of paints required to stay within tolerance is not known. At the Midwest Proton Radiotherapy Institute (MPRI) in Indiana, a design goal was to achieve a minimum of 100 paints per layer. Testing of a 10 cm diameter field with 8 nanoamperes (nA) of

proton current showed that the MPRI team was effectively able to reduce the number of paints on each layer from 100 to about 25-30. They found no discernible difference in transverse field uniformity [6]. This number of paints may not be equivalent between MPRI and ProCure NJ, as the scanning patterns are different between the two centers. ProCure NJ also uses ridge filters when applicable. A ridge filter is a small device that can spread out the first few layers of the treatment field. In proton radiotherapy with a cyclotron, a good portion of the beam time can be switching between layers. By being able to deliver up to the equivalent of 12 layers on the first layer, without switching energies 11 times, considerable time can be reduced from the patient treatment time.

The purpose of this research paper is to determine the minimum number of paints required on the first layer for patient treatment at ProCure, NJ, while staying within flatness and symmetry tolerance. Based on previous research [6], it seems plausible that 40 paints on the first layer could be reduced safely. By lowering the required number of paints on the first layer, the treatment time can be reduced for every field. Shorter treatment times can lead to less patient motion during treatment, which could result in more accurate treatments and more patient comfort.

Chapter 2

Materials and Methods

Different numbers of paints were simulated and measured to find the optimal number of paints on the first layer of the SOBP for patient treatment. I used the numerical computation software MATLAB to create a program to simulate the minimum number of paints necessary. The IC ProfilerTM Model 1122 at ProCure NJ was used to measure beam characteristics such as flatness and symmetry. The variables measured were numbers of paints, range and modulation combinations.

The MATLAB simulation uses a simple algorithm to determine the minimum number of paints that will cover the treatment field and still stay within our tolerance of flatness and symmetry. The simulation uses basic geometry, including the beam size and treatment field size, to simulate how much radiation accumulates within each pixel. The possible treatment field sizes at ProCure, NJ are $18 \times 18 \text{ cm}^2$ and $25 \times 25 \text{ cm}^2$. As a compromise between pixilation of the field and running time for the program, a field size of 540 (180 x 3) was chosen. This is represented in the program as a 540x540 cell matrix. The matrix is created with zeros to start.

2.1 Beam Size

At ProCure NJ, the beam size was measured before the start of this project for different ranges and modulations. The beam size is an average of roughly 2.2cm sigma \pm about 10% or 2.2mm [7]. This means that about 68.2% of the radiation is contained within a radius of 2.2cm, and that it follows a Gaussian curve. A 2-D Gaussian curve was modeled for the beam, with the central pixel at roughly a value of 1, and the outer pixels dropped as a function of distance from the central pixel. Therefore, at the edge of a beam of size 44x44 cells, the value of a cell at the edge of the beam is roughly 66% of the value of the central cell (one sigma away, or one-half the beam size). The beam is portrayed below:

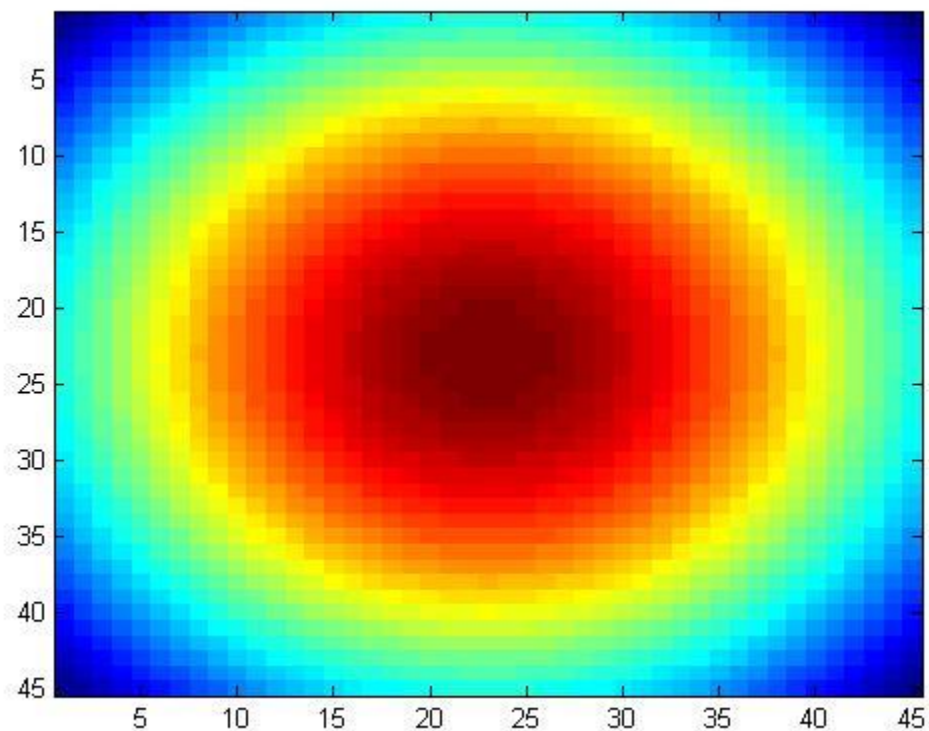


Figure 2.1 Simulated Beam. Above is a beam from the MATLAB simulation, with red signifying the maximum radiation (a value of ~ 1 in the program) and the blue signifying the minimum radiation.

This beam was created by using the Gaussian function in MATLAB code loop:

```
beam(i,j) = 2.5/(sigma*sqrt(2*pi))*exp((- (r-u).^2)/2*sigma^2);
```

where i and j are the indexes of the matrix, sigma is the standard deviation of the beam, and r is the distance from the central pixel. Because a radiation beam can be described as a Gaussian, standard deviation can describe the angular distribution [2] In this case, i and j= 1 to 44. The 2.5 factor at the start of the equation is simply to make the central pixel close to 1. 'r' is computed by taking the quadrature sum of the cell indexes, based on how far away they are from the center. The equation for "r" in MATLAB is below:

```
r = (1/middle)*sqrt((middle-i)^2 + (middle-j)^2);
```

where 'middle' is the central pixel. The (1/middle) factor sets the value of the pixel at the edge of the beam to 66% of the maximum.

2.2 Simulation

This simulated beam was scanned across an 18 x 18 cm² field with the same velocity and pattern that it is scanned at ProCure NJ. The pattern was discussed in the introduction, moving at 3 Hz in the horizontal direction, and 30 Hz in the vertical direction. The beam was scanned across the treatment field with various numbers of paints and random starting positions. After a set number of paints, the simulation would stop and then compute flatness and symmetry across the field. This data can also be visualized in a 2-D manner for qualitative analysis. The flatness and symmetry in the horizontal and vertical planes were analyzed with many different paints and random starting positions. One example of a typical treatment field is below:

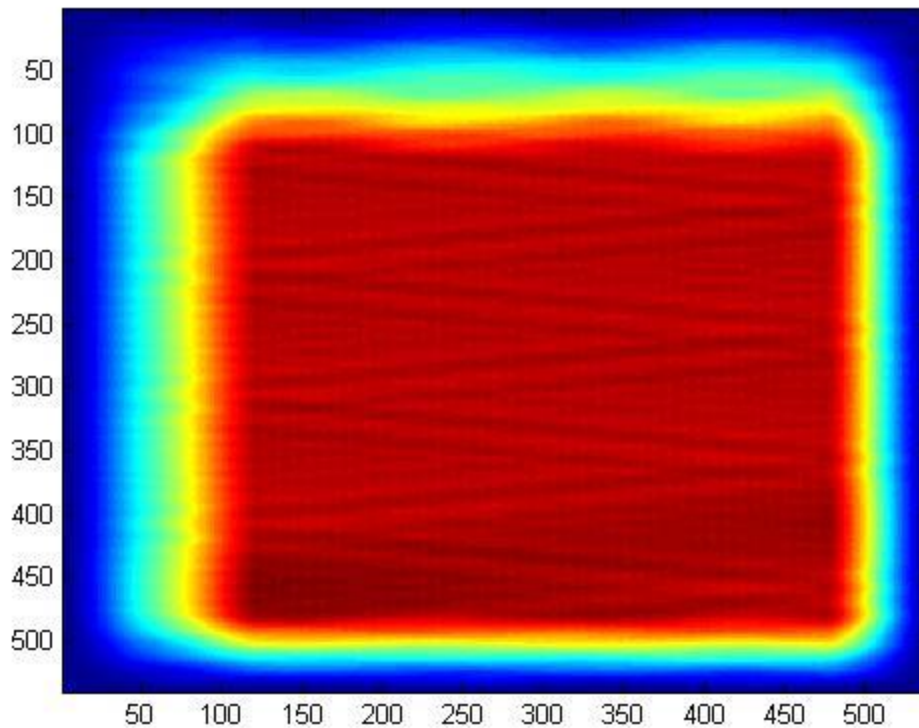


Figure 2.2 Untrimmed Field. The treatment field after scanning the beam across it 40 times. Red signifies the maximum radiation, blue signifies the minimum. In this case, the treatment field was represented by a 540x540 cell matrix. The axes seen above are the position in the treatment field matrix.

When the beam reaches the edge of the field, it is programmed to bounce the other way. Because of this programming choice, the center of the beam never reaches the edge of the field. The edge of the field in the simulation does not represent the clinical treatment beam, as the outer edges of the simulation field are significantly lower radiation than the central portion. The field is “trimmed” by a trimming function to better represent the clinical treatment beam. This function copies the useful inner portion of the matrix to a new matrix, and then the data is analyzed. The amount of the treatment field that is trimmed was derived empirically through

trial and error. Once the field appeared to have no border, the field was assumed to have been sufficiently trimmed. The following is a one-dimensional example of the trimming function: assume we have a vector of 10 cells (1x10, cells numbering 1, 2, ... 10). If the trimming value is set to 0.1, the first 10% and the last 10% of the vector is excluded from the trimmed vector. The trimmed vector will be eight cells, cell numbers two through nine. The trimming value for this study is 0.3. Below is a figure from MATLAB that has gone through the trimming function:

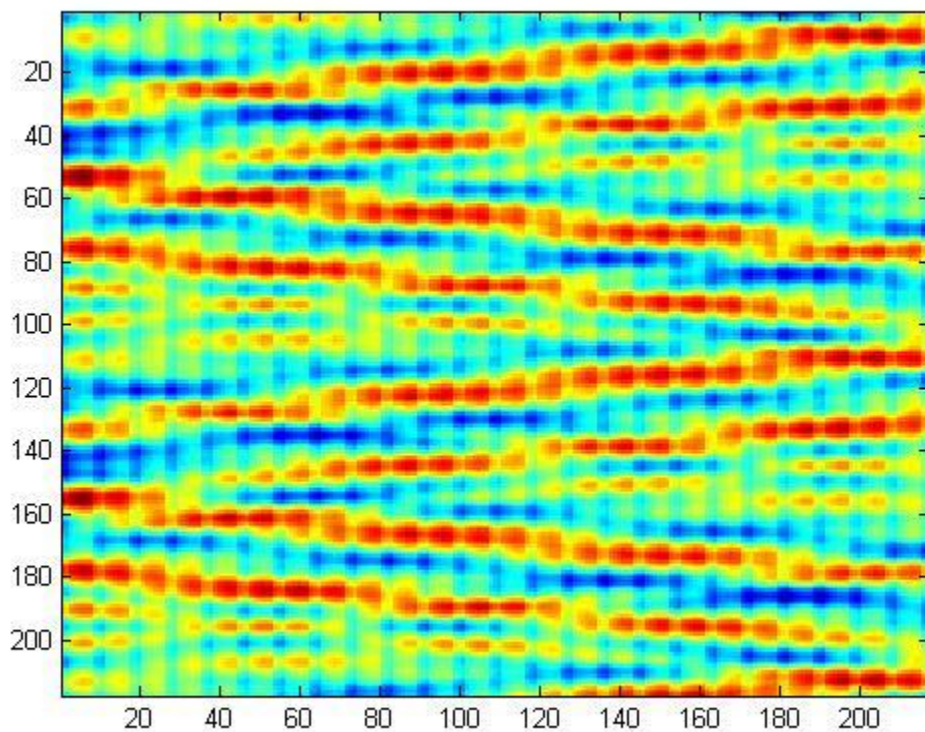


Figure 2.3 Trimmed Field. The treatment field after scanning the beam across it 40 times. Red signifies the maximum radiation, blue signifies the minimum. Although the field appears to be noisy, it is not. The calculated flatness and symmetry is within the specified tolerance (less than 2% symmetry, less than 3% flatness). This time, the inner portion of the field was copied to a new matrix to properly analyze the flatness and symmetry.

Because of the way the data is visualized by MATLAB, this data appears to be noisy, but it is in fact within clinical tolerance of flatness and symmetry. The simulation was written such that the “beam” is scanned faster in the horizontal direction rather than the vertical direction. Because the beam should be symmetric in the horizontal and vertical directions, this difference can be ignored. Another reason the scanning direction is inconsequential is because all statistics are calculated in the x and y directions.

2.3 Flatness and Symmetry

The definitions of flatness and symmetry will follow the convention of The Journal of International Commission on Radiation Units and Measurements (ICRU) report number 78. The report states:

Lateral flatness (in percent) is defined as

$$F_{lp} = \frac{(d_{lp \max} - d_{lp \min})}{(d_{lp \max} + d_{lp \min})} \times 100,$$

where $d_{lp \max}$ and $d_{lp \min}$ are the maximum and minimum absorbed dose values in the beam profile measured in the target width.

Lateral symmetry (in percent) is defined as

$$S_{lp} = \frac{(D_1 - D_2)}{(D_1 + D_2)} \times 100,$$

where D_1 and D_2 are the integrated absorbed doses in each half of the field about the central axis.

2.4 Measurements

All measurements were taken at ProCure, NJ using the Sun Nuclear IC ProfilerTM Model 1122. The IC Profiler contains 251 parallel plate ion chamber detectors. These ion chambers are organized into four linear arrays: an X axis, a Y axis, and two diagonal axes. The detectors on the X and Y axes have a spacing of 5mm; the diagonal axes have a spacing of 7.07mm [7]. The lateral field size of the IC Profiler is 32 x 32 cm². Currently (as of February 2013), the largest possible field size deliverable to isocenter clinically is approximately a 30cm diameter circle, making the IC Profiler a suitable device for all field sizes. The Sun Nuclear software for the IC Profiler has the ability to capture up to 8 frames per second.

The IC Profiler measurements were taken in air using different amounts of Plastic Water. Plastic Water is an approximation used in radiation measurements to reproduce results similar to radiation measurements taken in a water tank with water. ProCure NJ has Plastic Water slabs of varying thickness. The snout protrudes from the wall and shoots the beam of protons directly horizontal into the Plastic Water, and then the IC Profiler. At ProCure, NJ, there are different treatment rooms that can treat at different angles, but for this study, only the horizontal treatment angle will be discussed and measured. This beam will first hit the Plastic Water, accounting for the build-up region. The IC Profiler is placed behind varying amounts of solid water, and will measure the desired beam statistics. For ease of measurement, the IC Profiler was always placed at the center of the SOBP.

All of the measurements were taken on the 18 cm snout. The 18 cm snout was chosen for a few reasons: (1) because it represents a middle ground between the 10 cm and 25 cm snouts (the two other current treatment snouts at ProCure, NJ), (2) because the beam statistics will be

better than the 10 cm snout (fewer ion chambers in the field lead to less data, or larger noise), and (3) the data should theoretically be the same regardless of snout size. As described before, range describes how far the beam of protons penetrates a medium. Modulation describes the flat region of the SOBP. The following ranges and modulations were used:

Range (g/cm²)	Modulation (g/cm²)
10	5
15	10
17	10
19	10
29	10

Table 2.1. The range and modulation values chosen for this study.

While using these ranges and modulations, the air gap remained constant at 10 cm. Air gap is defined as the distance from the edge of the aperture to the front of the Plastic Water. To do this, the snout position (which is defined as the downstream edge of the aperture to isocenter) changes for every range and modulation combination. These ranges and modulations were chosen because they were used in the initial characterization of the flatness and symmetry of each room at ProCure NJ.

Chapter 3

Results

3.1 Simulation

The MATLAB simulation was run a total of 588 times with varying numbers of paints.

Below is a table and graph of the results:

Paints	# Passes	# Tests	Pass Rate
50	96	100	96%
40	94	124	76%
30	116	200	58%
20	60	164	37%

Table 3.1 Number of Paints, Passing Rate

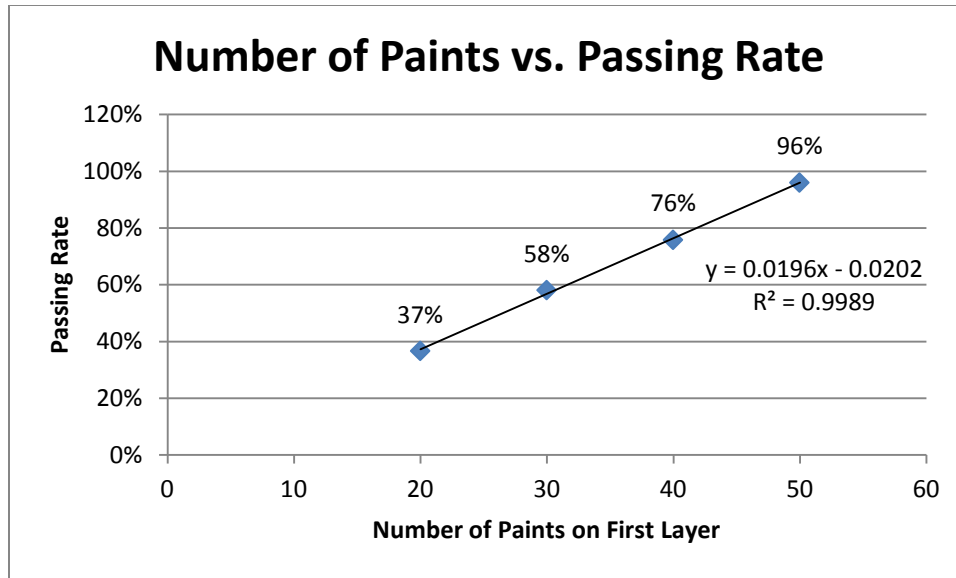


Figure 3.1 Number of Paints vs. Passing Rate. The above figure shows the number of paints on a layer vs. the percentage of simulations that passed.

The simulation was run many times at varying numbers of paints and follows a linear fit very well, with the coefficient of determination (R^2) being 0.9989. The starting position for every run was randomly chosen. The reason for choosing a random starting position is twofold: (1), the simulation will produce exactly the same results if the beam has the same starting position every time, and (2), the clinical beam has a random starting position for every beam delivered. The following code produced a random starting position:

```
x = round(rand(1)*fieldSize)-beamSize; %random beam starting position
y = round(rand(1)*fieldSize)-beamSize; %must be top left corner
if x < 1, x=1; end
if y < 1, y=1; end
```

The round() rounds to the nearest integer. For example, round(2.5) will return a value of 3. The round function was used because the starting position must be an integer. Because the beam is defined at the top left corner of the beam, the maximum starting in x or y must be the

size of the treatment field minus the size of the beam. Also, this function would sometimes define a starting position that is less than one. If this was the case, the starting position was forced to be one. This may produce a bias towards starting near the top left corner of the treatment field, but that should have very little bearing on the results of the flatness and symmetry. In the 588 simulations, 5 of the simulations started at (1,1). This bias will cause less than a one percent effect on the pass/fail results.

3.2 Measurements

Five sets of measurements were taken. Ranges 10, 15, 17, 19 and 29 were each measured five times while using 30 points for the first layer. The tolerance for flatness is $< 3\%$, and the tolerance for symmetry is between -2% and $+2\%$. The results show that the flatness and symmetry are within tolerance for the lower ranges (10, 15, 17, 19). Flatness was out of tolerance for all five measurements at range 29. All measurements were within tolerance for symmetry. Below are two figures of the results:

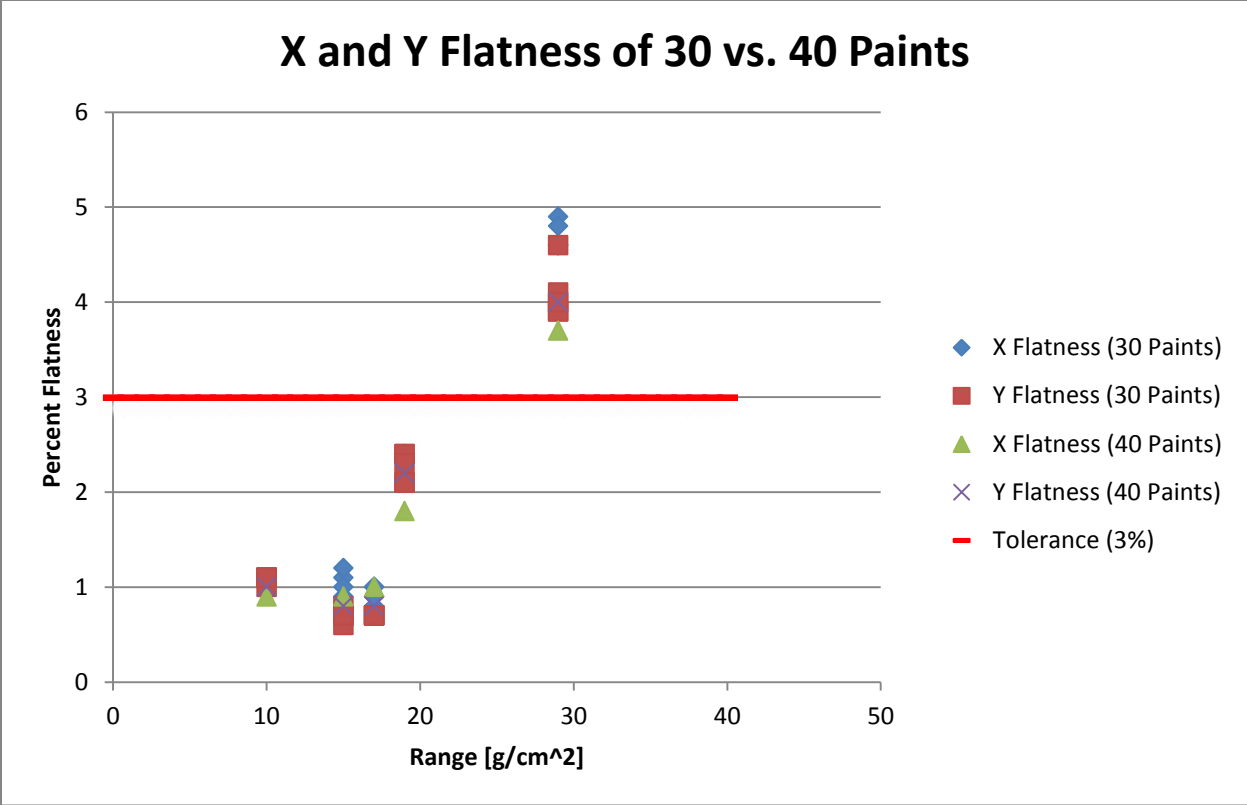


Figure 3.2 X and Y Flatness of 30 vs. 40 paints on the first layer.

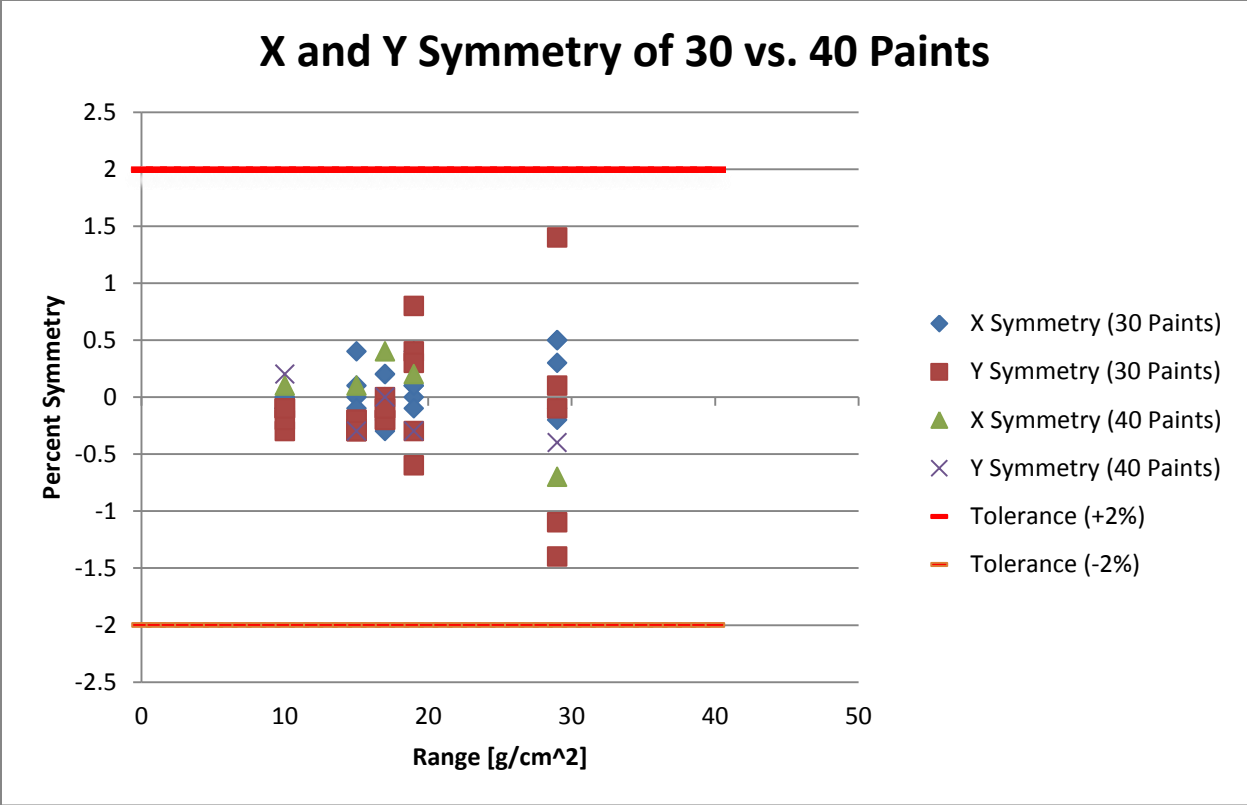


Figure 3.3 X and Y Symmetry of 30 vs. 40 paints on the first layer.

Chapter 4

Discussion

There are two sets of results that will be discussed. The first section will describe how well the simulation matches the measurements. The second section will describe how the measurements might be applied to patient treatments.

4.1 Measurement Versus Simulation

The purpose of this simulation is to model the first layer of the radiation field with varying numbers of paints. Because the number of paints is directly proportional to the patient treatment time, both the center (ProCure, NJ) and the patient will benefit from optimizing the number of paints on the first layer. The optimal number of paints on the first layer will be the minimum number of paints with flatness and symmetry within tolerance. Tolerance for flatness is to be less than 3%, and tolerance for symmetry is to be less than |2%|.

Ideally, we would like to measure 12 range/modulation combinations, repeating at least 5 times for reproducibility, on 3 different snouts, for at least 20, 30 and 40 paints on the first layer. Unfortunately, this adds up to $(12 \times 5 \times 3 \times 3)$ a minimum of 540 measurements. Beam time at ProCure NJ is currently very difficult to obtain, therefore it is not currently feasible to make this

vast number of measurements. The problem of beam time at ProCure, NJ has led to the development of this MATLAB simulation. Because it is not feasible to run all of the beam measurements, ideally the simulation would reproduce the results of our measurements. Once the program begins to model the beam characteristics well, it could possibly be used to predict which range/modulation/paint combinations would produce treatment fields within tolerance. With these predictions, the number of measurements necessary to make a clinical change could be significantly reduced.

The simulation shows a trend that we would expect. A higher number of paints shows a higher passing rate for flatness and symmetry. It is expected that 50 paints has a high passing rate (though it was not measured). The simulation showed that 40 paints have a 76% pass rate, which matches well with the measurement of 80% pass rate. Because of time constraints and lack of beam availability, only 5 measurements were made at the 40 paints setting, which might be too small a sample size to make any conclusions. Again, it is expected that 30 paints will have an even lower pass rate, and the simulation shows that the pass rate is 58%. Twenty-five measurements were taken with the 30 paints setting, so the statistics should be better than the 40 paints measurements. The pass rate based on measurements for 30 paints is 80%, which does not agree very well with the simulation. One would expect that the pass rate of 40 paints and 30 paints should *not* be the same, whereas the measurements show that they are.

4.2 The Influence of Range

Unfortunately, it appears that there is a more significant trend based on the range and modulation, rather than the number of paints. Only five sets of range and modulation combinations were tested, even though 30 paints were tested five times each. Regardless of the

number of paints measured, range 29 g/cm^2 did not pass. There are not input factors in the program for range and modulation, but there is an input for beam size. While the program models the number of paints well, it lacks the sophistication to model the range and modulation in a useful way. The program can give a general idea of the optimal number of paints based on an average range and modulation, but it does not currently give results based on different range and modulation combinations. Creating a simulation to model the range and modulation of the beam is beyond the scope of this paper. A simulation that models range and modulation might be appropriate for a further study, or possibly a Master's of Science thesis.

Based on the measurements, it appears that the lower ranges are well within tolerance for flatness and symmetry. Ideally, more range and modulation combinations would be used, as well as different snout sizes and different numbers of paints on the first layer. However, beam time for research at ProCure NJ is currently very low. More testing is needed, but it appears that the number of paints on the first layer can be lowered for non-large ranges ($< 29 \text{ g/cm}^2$). Because of the way the Treatment Control Software (TCS) is maintained, it is possible to have different numbers of paints on the first layer for different range and modulation combinations. If it is shown that the larger ranges are out of tolerance in flatness, one solution may be to deliver the larger ranges using 40 paints on the first layer, and the smaller ranges may be delivered with fewer paints on the first layer. Unfortunately, the range and modulation is not modeled by the simulation.

Chapter 5

Future Studies

For future studies, it is obvious that more measurements are needed. While developing the simulation may better define which measurements need to be made, one could also say that there need to be more measurements to direct the simulation. Once more measurements are made, a clearer understanding of how range and modulation affect the flatness and symmetry of the beams can be obtained.

Chapter 6

References

- [1] R. Slopesma, Proton Therapy Physics, H. Paganetti, Ed., Boca Raton, FL: CRC Press, Taylor & Francis Group, 2012.
- [2] F. Kahn, The Physics of Radiation Therapy, Philadelphia: Lippincott Williams & Wilkins, 2003, p. 42.
- [3] V. Anferov, "Scan Pattern Optimization for Uniform Proton Beam Scanning," *Journal of Medical Physics*, pp. 3560-3567 (3560), 2009.
- [4] H. S. Y. A. G. G. M. G. N. K. R. M. H. T. H. T. S. V. D. Jones, Prescribing, Recording, and Reporting Proton-Beam Therapy, Oxford, UK: Oxford University Press, 2007, p. 44.
- [5] T. Akagi, "Ridge Filter Design for Proton Therapy at Hyogo Ion Beam Medical Center," *Physics, Medicine & Biology*, vol. 48, pp. N301-N312, 2003.
- [6] A. M. W. H. C. A. F. J. A. S. M. W. D. N. V. A. J. B. Farr, "Clinical Characterization of a Proton Beam Continuous Uniform Scanning System with Dose Layer Stacking," *The Journal of Medical Physics*, vol. 35, no. 11, pp. 4945-4954, 2008.
- [7] T. Simon, "Characterization of a Multi-Axis Ion Chamber Array," *Journal of Medical Physics*, vol. 37, no. 11, pp. 6101-6111, 2010.